Journal Pre-proof

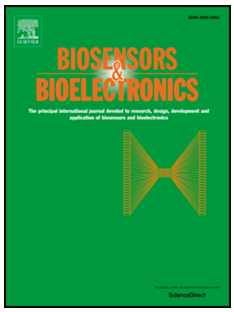

Electrochemical sandwich-type thrombin aptasensor based on dual signal amplification strategy of silver nanowires and hollow Au–CeO_2

Qiaoxia Zhang, Gaochao Fan, Wei Chen, Qing Liu, Xiao Zhang, Xianxi Zhang, Qingyun Liu

PII: S0956-5663(19)30925-X

DOI: https://doi.org/10.1016/j.bios.2019.111846

Reference: BIOS 111846

To appear in: *Biosensors and Bioelectronics*

Received Date: 3 August 2019

Revised Date: 31 October 2019

Accepted Date: 1 November 2019

Please cite this article as: Zhang, Q., Fan, G., Chen, W., Liu, Q., Zhang, X., Zhang, X., Liu, Q., Electrochemical sandwich-type thrombin aptasensor based on dual signal amplification strategy of silver nanowires and hollow Au–CeO_2, *Biosensors and Bioelectronics* (2019), doi: https://doi.org/10.1016/j.bios.2019.111846.

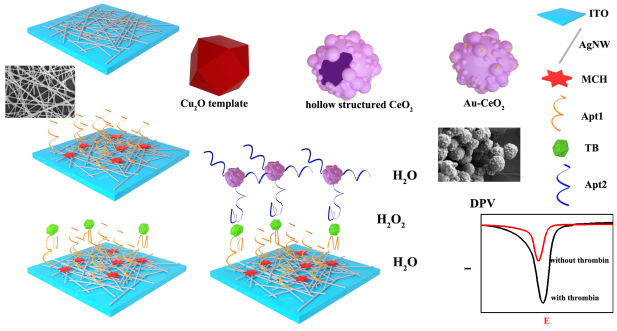

Electrochemical sandwich-type thrombin aptasensor based on dual signal amplification strategy of silver nanowires and hollow Au-CeO_2

Qiaoxia Zhang[a], Gaochao Fan[c], Wei Chen[a], Qing Liu[a], Xiao Zhang[c], Xianxi Zhang[b] and Qingyun Liu[a,*]

[a] *College of Chemical and Environmental Engineering; State Key Laboratory of Mining Disaster Prevention and Control Co-founded by Shandong Province and the Ministry of Science and Technology, Shandong University of Science and Technology, Qingdao 266590, China*

[b] *Shandong Provincial Key Laboratory/Collaborative Innovation Center of Chemical Energy Storage & Novel Cell Technology; School of Chemistry and Chemical Engineering, Liaocheng University, Liaocheng 252059, China*

[c] *College of Chemistry and Molecular Engineering, Qingdao University of Science & Technology, Qingdao 266042, China*

*Corresponding author. Tel: +86 0532 86057757; Fax: +86 0532 80681197

E-mail address: qyliu@sdust.edu.cn

Abstract:

Signal amplification is crucial in electrochemical biosensor to obtain low detection limits. In this work, a highly sensitive sandwich-type thrombin aptasensor is constructed, based on dual signal amplification of uniform silver nanowires (AgNWs) and hollow Au-CeO_2 nanocomposites. AgNWs are decorated on the ITO surface to immobilize amino functionalized thrombin capture apemeter 1 (Apt1). And Au nanoparticles (AuNPs) grown directly on the surface of hollow CeO_2 microstructure are used to immobilize sulfydryl functionalized thrombin reporter apemeter 2 (Apt2). Thus, sandwich-type apatasensor has been successfully designed, due to the specific recognition between thrombin and the two kinds of aptamers. One of the signal amplifications is from the good conductivity of uniform AgNWs. Moreover, uniform AgNWs together with hollow Au-CeO_2 exhibit the good catalytic performance for the reduction of H_2O_2, further resulting in significant electrochemical signal amplification. Because the electrochemical signal amplification is closely related to the thrombin concentration, differential pulse voltammetry is used to specifically detect thrombin. Under the optimized conditions, the proposed method has a good linear response ranged from 0.5 pM to 30 nM with a low detection limit of 0.25 pM (S/N = 3) for thrombin. The proposed thrombin aptasensor displays good selectivity, reproducibility and stability, providing a good platform for the ultrasensitive detection of thrombin.

Keywords: Electrochemical aptasensor; Sandwich-type; Thrombin; Au-CeO_2; Silver nanowires

1. Introduction

Thrombin, as a kind of allosteric serine protease, is not existed in blood under normal conditions. When vascular injury occurred, thrombin is rapidly generated from inactive zymogen prothrombin by a series of enzyme cleavages. Activated thrombin cleaves fibrinogen into fibrin and clots are formed at the site of vascular injury to prevent bleeding (Deng et al. 2014). Furthermore, thrombin plays an increasingly significant role in various pathological activities, such as coagulopathy, atherosclerosis, and cancer (Grover and Mackman 2018; Jennings 2009). Therefore, it is necessary to develop an effective method for highly selective and specific detection of thrombin in clinical diagnosis.

Aptamers are usually oligonucleotides or peptide bio-receptors, which are designed to specifically bind to the target substances. In comparison to traditional antibodies (Song et al. 2008; Xie et al. 2019), aptamers are widely used to develop aptasensors in biomedical diagnostics, due to its small size, chemical stability, cost effectiveness and easy modification for labeling or immobilization (Roushani and Shandost-fard 2016; Shandost-fard and Roushani 2017; Shandost-fard et al. 2014). In recent years, many biosensors based on aptamers have been developed for the detection of thrombin (Hao et al. 2018; Munzar et al. 2018). Among them, the electrochemical sandwich-type aptasensors using aptamer pairs have been extensively studied, because of their enhanced sensitivity and specificity. Especially, in order to realize the signal amplification, aptasensors are usually constructed with the aid of nanomaterials possessing catalytic activities, such as Au@Pd (Xu et al. 2015a),

PtNPs@Co(II)MOFs@PtNPs (Yang et al. 2017b), PtNPs/CNCs (Gao et al. 2016) and Cu_2O (Chen et al. 2018a; Zhao et al. 2017).

As a typical kind of one-dimensional nanomaterials, AgNWs possess their unique electrical, catalytic, physical and chemical properties. Notably, the unique structure can facilitate faster electron transfer between electrodes and analytes to promote the catalyzed processes, resulting in the sensitive improvement of electrochemical sensors (Lee et al. 2016). Moreover, it can be used as the biomolecule platform via Ag-N or Ag-S bonds (Zhou et al. 2018) for the immobilization of aptamers. In comparison to other noble metals (Au, Pt and Pd), another advantage is that Ag is highly abundant in earth crust and inexpensive (Devasenathipathy et al. 2017). Based on the previous investigations (Kumar-Krishnan et al. 2016; Nair et al. 2018), AgNWs are verified to exhibit the excellent catalytic performance for the reduction of H_2O_2. Thus, the AgNWs are selected as good substrate materials to modify the electrode.

The signal of the sandwich-type aptasensor usually can be amplified by the functional materials combined with the second aptamer (Fan et al. 2015). According to the previous study, CeO_2 can effectively catalyze the reduction of H_2O_2 (Yang et al. 2017a). The coexistence of Ce^{3+} and Ce^{4+} endows CeO_2 with superior redox activity, making the CeO_2 become a direct redox mediator to generate detectable electrochemical signal (Kibis et al. 2017). For the decoration of functional nanomaterials, Au has attracted considerable interests due to its superior auxiliary catalytic activity towards the reduction of H_2O_2 (Meng et al. 2011) and advantages of

good biocompatibility (Ye et al. 2017). And after CeO_2 was decorated with Au, the obtained Au-CeO_2 can be used to bind sulfydryl functionalized aptamer through Au-S bonds. As is known, the performance of nanomaterials is closely dependent on the morphology in different fields. Especially, hollow nano-/micro-structured materials have attracted considerable attention in the catalytic field (Wu et al. 2019), owing to their great specific surface area, low density, and more active sites. However, to the best of our knowledge, the combining dual signal amplification strategy of AgNWs and hollow Au-CeO_2 in the sandwich-type thrombin aptasensor has not been reported to thus far. Inspired by these, if a sandwich-type thrombin aptasensor based on the dual signal amplification strategy of silver nanowires and hollow Au-CeO_2 is constructed for the reduction of H_2O_2, it will be a good attempt for the detection of thrombin with high sensitivity and selectivity.

Herein, uniform AgNWs and hollow Au-CeO_2 are introduced to construct the sandwich-type thrombin aptasensor with dual signal amplification. Uniform AgNWs were prepared by the polyol method and then were decorated onto the ITO electrode by a dipping method to facilitate electron transfer and improve the conductivity. Hollow Au-CeO_2 was introduced on the electrode through the assistance of sandwich-type structure. With the existence of H_2O_2 in the working buffer, both AgNWs and Au-CeO_2 can catalyze the H_2O_2 reduction, resulting in the dual signal amplification. Thus, an excellent electrochemical aptasensor has been constructed for the sensitive detection of thrombin.

2. Material and methods

2.1. Reagents and apparatus

All electrochemical measurements were carried out on a CHI760E electrochemical workstation (Shanghai Chenhua Instruments Co., Ltd, China). A conventional three-electrode system was used for all electrochemical measurements, consisting of a platinum plate as the counter electrode, a saturated calomel electrode (SCE) as the reference electrode. The other details are provided in Supplementary Material.

2.2 Preparation of AgNWs

AgNWs were synthesized according to a simple polyol method with a little modification (Zhang et al. 2015). The detailed preparation process was presented in Supplementary Material.

2.3 Preparation of hollow structured CeO_2

Hollow CeO_2 was prepared by the template method according to the previous study with a little modification (Ge et al. 2017). The detailed preparation process was presented in Supplementary Material.

2.4 Preparation of Au-CeO_2

AuNPs were in situ generated on hollow CeO_2 by the redox reaction according to

the published work with a little change (Zhang et al. 2012). The detailed preparation process was presented in Supplementary Material.

2.5 Preparation of Apt2-Au–CeO_2

10 mg synthesized Au-CeO_2 was dispersed in 5 mL tris-HCl solution (20 mM). After that, 500 μL 2.0 μM Apt2 was added and cultivated at 4 □ for 12 h. Thus, Apt2 was attached onto the Au-CeO_2 via Au-S bonds. After incubation, the product was centrifuged and washed with washing buffer to get rid of the free aptamer existed in the solution. Finally, the product was re-suspended in 5 mL tris-HCl (20 mM) and stored in 4 □ for the subsequent experiments.

2.6 Fabrication of the aptasensor

Firstly, The ITO electrode was sequentially ultrasonically cleaned with water, isopropanol, and acetone for 15 min, respectively. Then, the electrode was dried in nitrogen atmosphere. Secondly, the as-prepared AgNWs suspension was sonicated for 2 min to minimize the agglomeration of nanowires. The ITO electrode was vertically immersed in the AgNWs suspension and dried at 40 □. This process was repeated to obtain desired layer numbers (1, 2, 3, 4 and 5). After that, AgNWs were successfully loaded on the ITO electrode. To fuse the connecting junctions between nanowires, the AgNWs modified ITO electrode was heated at 200 □ in N_2 atmosphere for 20 min. Thirdly, 20 μL Apt1 (2.0 μM) was dropped on the AgNWs modified ITO electrode, covered with a plastic seal, and then incubated for 16 h at room temperature. Fourthly,

the electrode was vertically immersed in 0.5 mM MCH for 40 min to block nonspecific binding. Fifthly, 10 μL TB with different concentration was dropped on the electrode and incubated for a certain time (20, 30, 40, 50 and 60 min). Finally, 5 μL Apt2-Au–CeO_2 was dropped on the electrode, covered with a plastic seal, and then incubated for 2 h at room temperature. After each step, the electrode was washed with 10 mM PBS (pH 7.0) and finally the electrode was stored at 4 □, prior to the electrochemical measurements.

2.7 Electrochemical measurements

To investigate the stepwise fabrication of the working electrode, CV and EIS measurements were progressively carried out in a 5 mM $[Fe(CN)_6]^{3-/4-}$ solution containing 0.1 M KCl. The CV measurements were executed with a scan rate of 50 mV/s and a voltage range from −0.2 V to 0.6 V. The EIS parameters were a 5 mV amplitude and a frequency sweep from 0.1 to 10^6 Hz at room temperature. To study the concentration of TB, DPV was executed in PBS buffer containing 10 mM H_2O_2 as a sacrificial electron donor with the potential from 0.1 V to -0.4 V, amplitude of 0.05 V, pulse width of 0.05 s and pulse period of 0.5 s.

3. Results and discussion

3.1 The possible mechanism

The possible mechanism about this electrochemical biosensor is illustrated in

Scheme 1. AgNWs were decorated on the cleaned ITO surface and formed uniform conducting networks after immersion and heat treatment. This hierarchical networks facilitate the electron transfer, serving as both good conducting substrate and an enzyme-free electrochemical sensor for H_2O_2 (Chen et al. 2018b). What's more, AgNWs were used to immobilize thrombin capture probe (Apt1). The amino functionalized Apt1, which can specifically recognize TB, was immobilized on the surface of the AgNWs decorated ITO electrode by Ag-N bonds. The active surface area of the AgNWs/ITO electrode was calculated to be 0.7844 cm^2 and the detailed description was shown in Supplementary Material (Fig. S3). After the treatment with MCH, nonspecific bindings were removed. Subsequently, the immobilized Apt1 can specifically recognize the target TB. Moreover, due to the specific binding between TB and Apt2, Apt2–Au-CeO_2 was immobilized on the ITO electrode. Thus, both AgNWs and Au-CeO_2 co-contributed to the reduction of H_2O_2. During this process, sandwiched binding complexes drew catalytic labels Au-CeO_2 closely onto the surfaces of electrodes to generate amplified signal for detection (Deng et al. 2014). Therefore, they are applied to fabricate the sandwich-type electrochemical aptasensor for the sensitive determination of TB in the presence of H_2O_2.

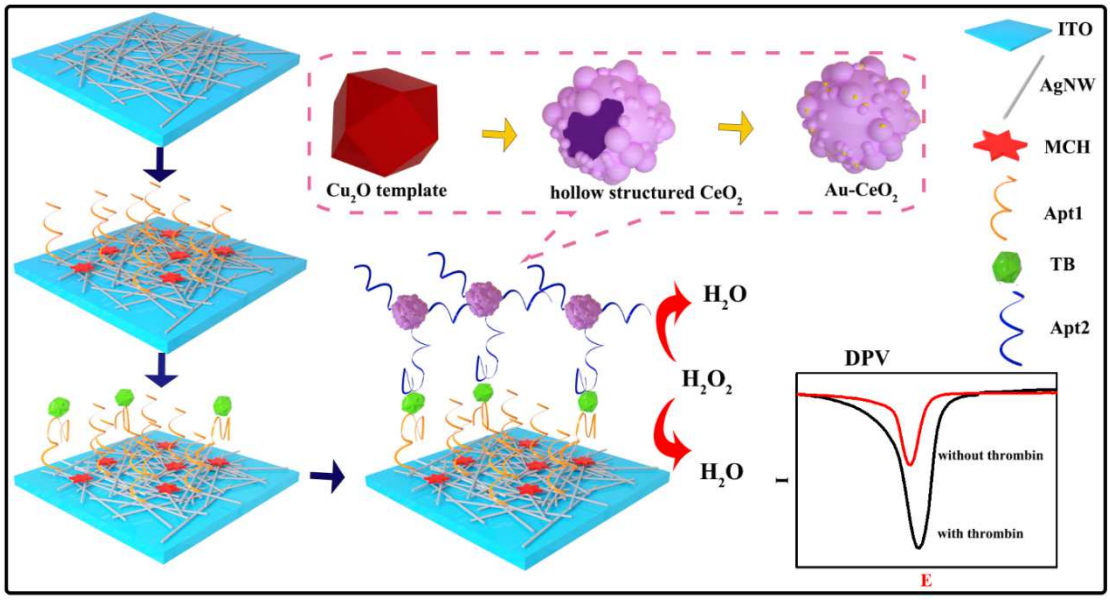

Scheme 1 The mechanism illustration of this electrochemical biosensor.

3.2 Characterization of as-prepared different materials

The morphologies of AgNWs, Cu_2O templates, CeO_2 and Au-CeO_2 are imaged by SEM. As shown in Fig. 1A, the uniform AgNWs are ca. 20 μm in length. From the inset of Fig. 1A, it can be found that the average diameter of the AgNW is approximately 80 nm. In the preparation of hollow CeO_2, Cu_2O template was used, shown in Fig. 2B. After removing the Cu_2O template, the hollow CeO_2 nanoboxes were obtained (shown in Fig. 1C), which copied the outline of Cu_2O template. Furthermore, it also can be found that many tiny particles assemble on the surface of CeO_2 nanoboxes. The unique structure brings more catalytic sites in favor of the reduction of H_2O_2 and more anchoring sites for Au nanoparticles. As can be seen from Fig. 1D, the decoration of Au nanoparticles has no obvious influence on the morphology of CeO_2.

To further study the morphology and composition of Au-CeO_2, the as-prepared

CeO_2 and Au-CeO_2 are also characterized by TEM. As displayed in Fig. 1E, the prepared CeO_2 displays a hollow structure with a relatively clear surface. After the decoration with Au, Au nanoparticles were coated on the surface of CeO_2 (Fig. 1F). From the HRTEM image (inset in Fig. 1F) of Au-CeO_2, it can be found that the 0.23 nm lattice spacing is corresponded to the (111) plane spacing of Au (Lee and Chen 2016), as well as the lattice fringes with 0.31 nm lattice spacing is consistent with the (111) plane spacing of CeO_2. It is suggested the successful formation of Au nanoparticles on the surface of hollow CeO_2.

The crystalline structures of prepared materials are analyzed by XRD. As shown in Fig. S1A, all diffraction signals of AgNWs are indexed to the face-centered cubic crystal structure (JCPDS No. 04-0783), indicating formation of the pure crystalline of AgNWs (Thirumalraj et al. 2016). As depicted in Fig. S1B, the diffraction signals of Cu_2O (JCPDS No. 05-0667) and CeO_2 (JCPDS No. 34-0394) samples can be found, suggesting that hollow CeO_2 is successfully prepared after Cu_2O templates were removed. Notably, after hollow CeO_2 was decorated with Au, a new diffraction peak at 2θ of about 38° appears in the diffraction patterns of Au-CeO_2, assigned to (111) crystal planes of Au (JCPDS No. 04-0784) (Alhumaimess et al. 2019).

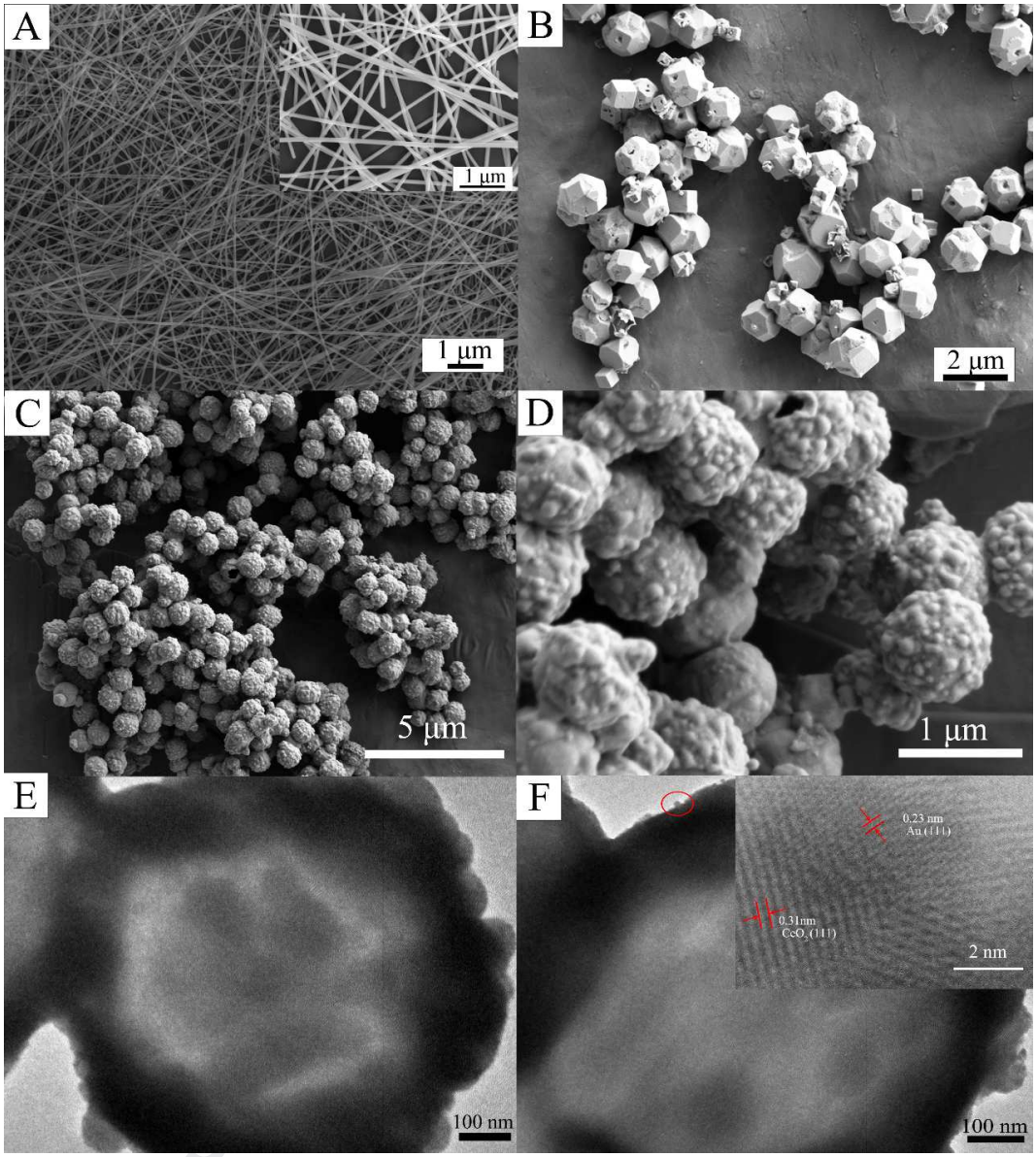

Fig. 1 SEM images of (A) AgNWs (Inset the enlarged SEM image of AgNWs), (B) Cu_2O, (C) CeO_2 and (D) Au-CeO_2; TEM images of (E) CeO_2 and (F) Au-CeO_2; HRTEM image of Au-CeO_2 (inset of F), respectively.

3.3 The electrochemical characterization of the stepwise modified electrodes

The CV and EIS measurements were carried out after each step of modification to characterize the interface properties of the electrodes. As is shown in Fig. 2A, a well-defined redox wave of $[Fe(CN)_6]^{3-/4-}$ is recorded on the surface of bare ITO

electrode. After the AgNWs were loaded on the ITO electrode, the redox peak current increases, due to the good electrical conductivity and high surface-to-volume ratio of AgNWs modified electrode (Lee et al. 2016). After the Apt1 was immobilized on the AgNWs/ITO electrode, the peak current decreases obviously. The reason is that the negatively charged phosphoric acid backbones of Apt1 impede the electron transfer of the redox couple. After the stepwise modified electrode with MCH and TB, the redox peak currents further decrease, because the bioactive substances can form an additional barrier on the surface of electrode. Furthermore, the redox peak decreases obviously after dealt with Apt2-Au–CeO_2, suggesting the formation of the sandwich-type of Apt1-TB- Apt2. That is because the bioactive substances can greatly inhibit the efficiency of electron transfer.

EIS is also used as an effective method to investigate the stepwise modified process of the electrodes in many works. The semicircle at higher frequencies of the Nyquist diagrams is associated with the electron transfer resistance (Ret), correlated with the modification of the electrode surface (Kavosi et al. 2015). As shown in Fig. 2B, compared with that of the bare ITO, the semicircle diameter of AgNWs/ITO electrode decreases, closely relating to the good conductivity of AgNWs. As expected, after the subsequent stepwise modification, the semicircle diameters increase gradually. The results are consistent with that of the CV data. Convincingly, all the results obtained above confirm that the designed detection platform has been successfully fabricated.

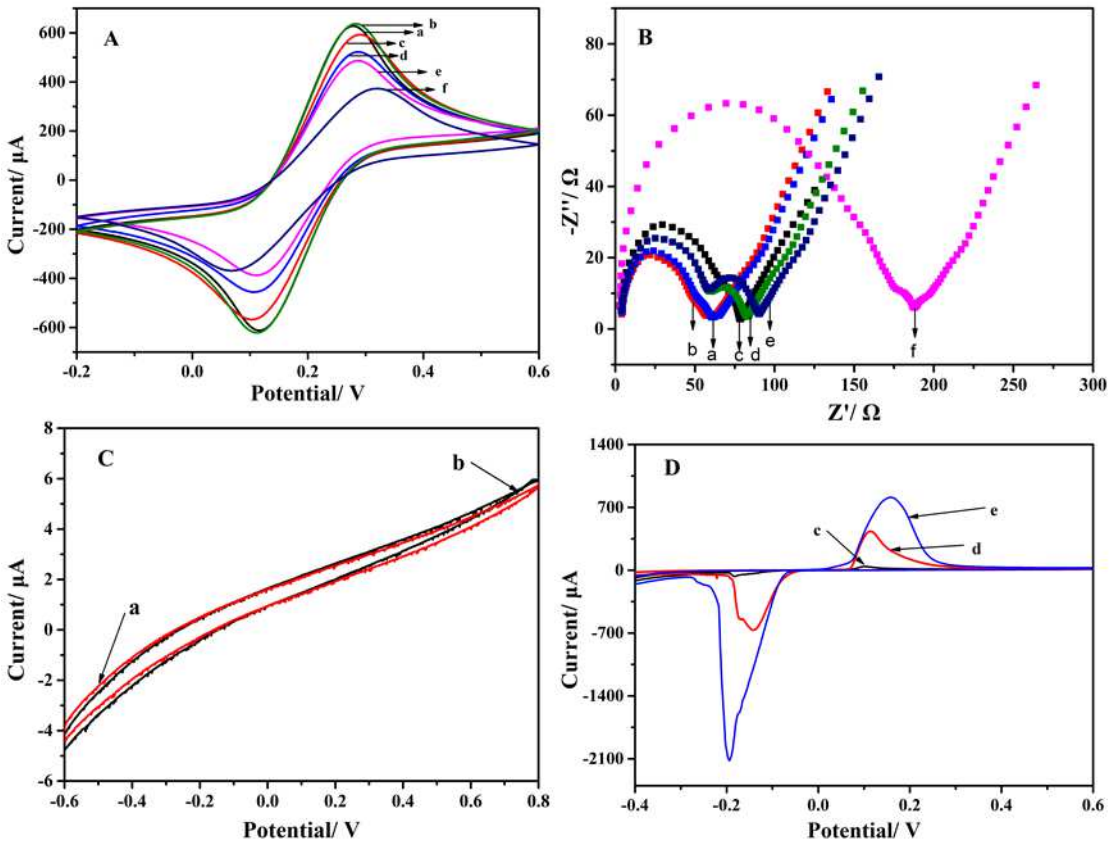

Fig. 2 (A) CV and (B) EIS responses of the different electrodes characterized in 5 mM $[Fe(CN)_6]^{3-/4-}$ solution containing 0.1 M KCl: (a) bare ITO, (b) AgNWs/ITO, (c) Apt1/AgNWs/ITO, (d) MCH/Apt1/AgNWs/ITO, (e) TB/MCH/Apt1/AgNWs/ITO and (f) Apt2–Au-CeO_2/TB/MCH/Apt1/AgNWs/ITO; (C, D) CV curves of the bare ITO (a and b), AgNWs/ITO electrode (c and d), and the final prepared Apt2–Au-CeO_2/TB/MCH/Apt1/AgNWs/ITO electrode (e) in PBS solutions in the absence of H_2O_2 (a and c) and in the presence of H_2O_2 (b, d and e), respectively.

3.4 The comparison of different signal probes

Cyclic voltammetry experiments were carried out to study the electrochemical behavior of H_2O_2 at different electrodes. Fig. 2C and Fig. 2D show CV curves of the bare ITO (a and b), AgNWs/ITO electrode (c and d), and the final prepared

Apt2–Au-CeO_2/TB/MCH/Apt1/AgNWs/ITO electrode (e) in PBS solutions in the absence of H_2O_2 (a and c) and in the presence of H_2O_2 (b, d and e), respectively. From smooth curves of (a) and (b), no obvious redox peaks of the bare ITO electrode are found with H_2O_2 or not. The CV curve of AgNW/ITO electrode (c) shows a slight redox peak in the absence of H_2O_2, because Ag was oxidized electrochemically to Ag (oxidation state), which was converted to Ag (reduction state) at the electrode surface in the reverse scan (Devasenathipathy et al. 2017). Upon existence of H_2O_2, a significant reduction peak can be observed (curve d). The increase of the cathodic current is attributed to the electro-reduction of H_2O_2 by AgNWs (Ahmad et al. 2015). Obviously, from curve e, it can be seen that the reduction current increases, indicating that the reduction of H_2O_2 is further improved by Apt2–Au-CeO_2/TB/MCH/Apt1/AgNWs/ITO electrode. The preliminary results suggest the possibility of TB detection based on the sandwich-type aptasensor.

3.5 Optimization of experimental conditions

To get better experimental conditions about the analytical performance for TB, several crucial factors, including dipping cycles, incubation time, concentration of Au-CeO_2 and pH of PBS were optimized. Various working electrodes were used to detect TB (10 nM) in different conditions. The DPV measurements were performed in the PBS solution containing 0.1 M KCl and 10 mM H_2O_2.

The dipping cycles of AgNWs can affect the electroconductivity of AgNWs/ITO electrode. As shown in Fig. 3A, five times of different cycles with a series of

AgNWs/ITO electrods are investigated. As the dipping cycles increase, the peak currents rise gradually and reach to the maximum at the 3rd cycle. H_2O_2 is reduced under the catalization by AgNWs deposited on the electrode surface. Thereby, with the increase amount of AgNWs on the electrode surface, the output current is increased (Kumar-Krishnan et al. 2016), which may be due to the increase of connection between AgNWs and the improvement of electrode surface area. Nevertheless, with further increases of dipping cycles, the electroconductibility of AgNWs is insufficient to significantly offset the contact resistance of the wires, resulting in that the charge transfer is restricted for the catalytic decomposition of H_2O_2 (Xu et al. 2015b). Thus, 3 dipping cycle is chosen as the optimum number for preparation of AgNWs/ITO electrode.

The incubation time of TB is another important parameter for the system, because the thrombin detection is dependent on the successful formation of Apt1-TB-Apt2 sandwich-type structure. As shown in Fig. 3B, when the duration of incubation time is up to 40 min, the current peak rises up to the maximum and then maintains steadily with the incubation time lasted from 40 to 60 min. Therefore, 40 min is the optimum incubation time of TB in this aptasensor.

The third important parameter is the concentration of Au-CeO_2 in the Apt2–Au-CeO_2 suspension. Because Au-CeO_2 can catalyze the reduction of H_2O_2, the suitable concentration of Au-CeO_2 is essential for the successful formation of reporter probe Apt2–Au-CeO_2. A suitable amount of Au-CeO_2 is important for the improvement of signal current in the sandwich-type aptasensor. As can be seen from

Fig. 3C, 2 mg/mL is selected as the optimum concentration of Au-CeO_2.

The analytical performance of this aptasensor is also closely related to the electrolyte pH values in the DPV measurement. Different pH values including 6.0, 6.5, 7.0, 7.5, 8.0 were used to explore the most suitable supporting electrolyte. As presented in Fig. 3D, the current is enhanced with the increase of the pH value from 6.0 to 7.0, while decreases from 7.0 to 8.0. Thus, pH=7.0 PBS solution is used as the working solution medium for the TB detection.

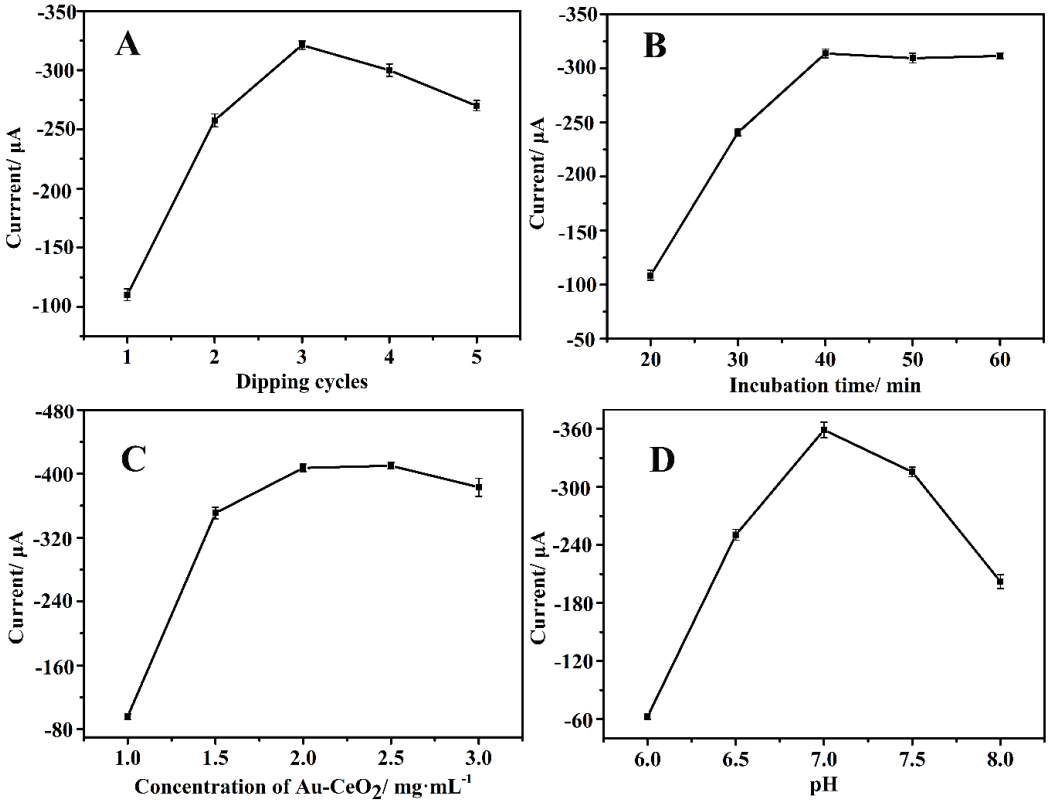

Fig. 3 Optimization of the experimental conditions: (A) dipping cycles of AgNWs, (B) incubation time of TB, (C) concentration of Au-CeO_2, and (D) pH value of electrolyte, respectively.

3.6 Analytical performance of the aptasensor

Under the optimized experimental conditions, the analytical performance of the proposed aptasensor was evaluated by measuring DPV responses of the aptasensors incubated with different concentrations of TB. As shown in Fig. 4A, the response peak current signal in DPV increases with the increase of TB concentration in the range of 0.0005 to 30 nM, which is wider than that of the sandwiched thrombin aptasensor based on WSe_2 and AuNPs (Wang et al. 2018). The corresponding regression equation is $I = -37.85\log C_{TB} - 388.09$ with a correlation coefficient of 0.9988, and the limit of detection (LOD) is calculated to be 0.25 pM (S/N = 3), which is lower than that of the aptasensor based on magnetic biocomposite Fe_3O_4@AuNPs (Zhu et al. 2019). As a comparison, the analytical performance of the proposed aptasensor is compared with some of other published strategies for TB detection, listed in Table 1. The outstanding analytical performance of the aptasensor may be attributed to the following reasons: Firstly, other than the successful immobilization of Apt1, AgNWs possess the remarkable electroconductibility, benefiting the electrons transfer towards the surface of the electrode and then resulting in the signal amplification. Secondly, AgNWs possessing the excellent catalytic activity in the reduction of H_2O_2, can further improve the electrical response signals in the detection of TB. Thirdly, the significant increase of the response signal is due to the synergistic effect between AgNWs and Au-CeO_2 for the catalytic decomposition of H_2O_2. Lastly, the unique structure of hollow Au-CeO_2 with a large specific surface area contributes to the superb catalytic performance for the reduction of H_2O_2, further enhancing the

electrochemical signal and then leading to a much higher sensitivity.

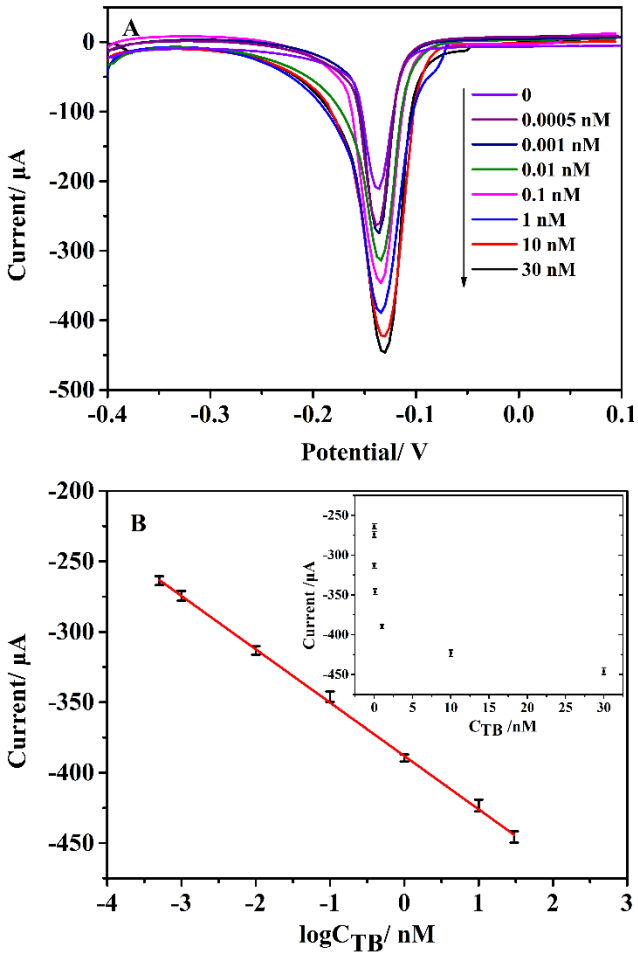

Fig. 4 (A) DPV responses of the aptasensor incubated with different concentrations of TB from 0.0005 nM to 30 nM (including C_{TB}=0) in PBS buffer (pH 7.0) containing 10 mM H_2O_2; (B) The calibration plots of DPV peak current versus the logarithm of TB concentration; DPV peak current versus the TB concentration (inset of Fig. 4B) (Error bar: SD, n=3).

Table 1 Comparison of several typical electrochemistry methods for thrombin detection.

Electrode+materials	Analytical technique	Linear range	LOD
GCE/WSe_2/AuNPs + AuNPs(Wang et al. 2018)	DPV	0.1 pM-20 nM	23 fM
GCE/AuNPs+PtNPs@Co(II)MOFs@PtNPs(Yang et al. 2017b)	DPV	0.1 pM–50 nM	33 fM
GCE/AuNPs+ Cu_2O-Au(Chen et al. 2018a)	Chronoamperometry	0.1 pM to 20 nM	23 fM
MGCE+Fe_3O_4@AuNPs(Zhu et al. 2019)	DPV	5 pM-5 nM	1.8 pM
GCE/AuNP-SN-GO+ AuNP-SN-GO(He 2018)	DPV	0.1 pM-10 nM	0.025 pM
ITO/AgNWs+Au-CeO_2(this work)	DPV	0.5 pM to 30 nM	0.25 pM

3.7 Selectivity, stability and reproducibility of the aptasensor

To investigate the specificity of the aptasensor, the DPV responses of three different interfering substances including L-cys, lysozyme, BSA together with TB and the mixture of these four kinds of substances have been comparatively investigated. As shown in Fig. S2A, compared with the blank signal, when the aptasensor is incubated with L-cys (10 nM), lysozyme (10 nM), BSA (10 nM), the electrochemical signal has little change. However, the electrochemical signal increases clearly after incubation with TB (1 nM). Furthermore, the same electrochemical signal value for the mixture of the above four substances is obtained, compared with that of apatsensor incubated with TB. These results indicate the high selectivity of the proposed aptasensor.

To study stability of the aptasensor, the fabricated aptasensor is stored at 4 □ for

a certain time. As depicted in Fig. S2B, after 10 days of storage, the electrochemical signal of the aptasensor shows a negligible change, compared with that in the first day. After 20 days of storage, the electrochemical signal still retains 92.52% of their initial electrochemical signal. The operational stability of this biosensor was also studied, shown in Fig S5. As can be found, after 20 repetitive cycles, no remarkable change (93.7% of the 1^{st} cycle value) was observed in the reduction peak current. The results of storage and operational stability study indicate the stability of the proposed aptasensor is acceptable. Furthermore, three different batches of working electrodes (each batch was composed with 5 replicated electrodes) incubated with 1 nM TB for the reproducibility and consistency study. The reproducibility was manifested through the relative standard deviations (RSDs) (marked in Fig. S2C) within the same batch. The relative standard deviation of all the samples is 1.16%, which indicated the aptasensor's consistency of different batches. The results suggest that the reproducibility and consistency of the proposed aptasensor are acceptable.

3.8. Real sample analysis

To further study the practicality of the proposed method, the recovery test is studied with the standard addition assay by adding different concentrations of thrombin into 10-fold-diluted human serum samples, summarized in Table S1 (in Supplementary Material). The recovery rate of this method ranges from 96.2% to 109% and RSDs is 1.34%–3.32%, suggesting that the proposed method can be applied in thrombin analysis of real samples.

4. Conclusions

In summary, an ultrasensitive electrochemical sandwich-type aptasensor for the sensitive and selective detection of TB based on dual signal amplification strategy of AgNWs and hollow Au-CeO_2 has been designed. These AgNWs benefit not only to bind biomolecules but also to improve the electron transfer, accompanied with signal amplification. Furthermore, both AgNWs and Au-CeO_2 can catalyze the reduction of H_2O_2, co-contributing to the signal amplification of the aptasensor. The proposed electrochemical platform has a great potential application in developing of various sensitive aptasensors for the detection of other disease-related proteins, only by replacing the thrombin aptamers with specific aptamers. As the complete regeneration of the aptamer-based layer is difficult to achieve, a typical limitation of this method was the proposed aptasensors are single-use. And there are still much more efforts should be given to improve the preparation protocol of aptamer-sensing layer for the point-of-care system.

Acknowledgement

This work was supported by the National Natural Science Foundation of China (Grant No. 21971152 and 21805168), Natural Science Foundation of Shandong Province (Grant No. ZR2018MB002, ZR2018MEE003, ZR2018PEE006 and ZR2017BB046), Scientific Research Foundation of Shandong University of Science and Technology for Recruited Talents (Grant No. 2015RCJJ018, 2017RCJJ040 and 2017RCJJ041), Shandong Key Laboratory of Biochemical Analysis (SKLBA1909)

and the Science and Technology Projects for Colleges and Universities in Shandong Province (J17KA097).

References

Ahmad, M., Sun, H., Hussain, M., Karim, S., Nisar, A., Khan, M., 2015. Electroanalysis 27(6), 1498-1506.

Alhumaimess, M., Aldosari, O., Alshammari, H., Kamel, M.M., Betiha, M.A., Hassan, H.M.A., 2019. J. Mol. Liq. 279, 649-656.

Chen, S., Liu, P., Su, K., Li, X., Qin, Z., Xu, W., Chen, J., Li, C., Qiu, J., 2018a. Biosens. Bioelectron. 99, 338-345.

Chen, Y.C., Hsu, J.H., Hsu, Y.K., 2018b. Microchim. Acta 185(2), 106.

Deng, B., Lin, Y., Wang, C., Li, F., Wang, Z., Zhang, H., Li, X.F., Le, X.C., 2014. Anal. Chim. Acta 837, 1-15.

Devasenathipathy, R., Liu, Y.X., Yang, C., Rani, K.K., Wang, S.F., 2017. Sens. Actuators, B 252, 862-869.

Fan, H., Guo, Z., Gao, L., Zhang, Y., Fan, D., Ji, G., Du, B., Wei, Q., 2015. Biosens. Bioelectron. 64, 51-56.

Gao, F., Du, L., Zhang, Y., Zhou, F., Tang, D., 2016. Biosens. Bioelectron. 86, 185-193.

Ge, S., Bao, L., Shao, Q., Zhang, Q., Liu, Q., 2017. J. Nanosci. Nanotechnol. 17, 833-836.

Grover, S.P., Mackman, N., 2018. Arterioscler., Thromb., Vasc. Biol. 38(4), 709-725.

Hao, N., Hua, R., Chen, S.B., Zhang, Y., Zhou, Z., Qian, J., Liu, Q., Wang, K., 2018. Biosens. Bioelectron. 101, 14-20.

He, B.S., 2018. Microchim. Acta 185(7), 344.

Jennings, L.K., 2009. Thromb. Haemostasis 102(2), 248-257.

Kavosi, B., Salimi, A., Hallaj, R., Moradi, F., 2015. Biosens. Bioelectron. 74, 915-923.

Kibis, L.S., Kardash, T.Y., Derevyannikova, E.A., Stonkus, O.A., Slavinskaya, E.M., Svetlichnyi, V.A., Boronin, A.I., 2017. J. Phys. Chem. C 121(48), 26925-26938.

Kumar-Krishnan, S., Chakaravarthy, S., Hernandez-Rangel, A., Prokhorov, E., Luna-Barcenas, G., Esparza, R., Meyyappan, M., 2016. RSC Adv. 6(24), 20102-20108.

Lee, D.S., Chen, Y.W., 2016. Int. J. Hydrogen Energy 41(5), 3605-3612.

Lee, J.H., Lee, H., Huynh-Nguyen, B.-C., Ko, E., Kim, J.H., Seong, G.H., 2016. Sens. Actuators, B 224, 789-797.

Meng, F., Yan, X., Liu, J., Gu, J., Zou, Z., 2011. Electrochim. Acta 56(12), 4657-4662.

Munzar, J.D., Ng, A., Juncker, D., 2018. Nat. Commun. 9, 343.

Nair, A.K., Nair, K.M.S., Thomas, S., Rouxel, D., Alwarappan, S., Kalarikkal, N., 2018. Langmuir 34(45), 13603-13614.

Roushani, M., Shandost-fard, F., 2016. Mater. Sci. Eng., C 68, 128-135.

Shandost-fard, F., Roushani, M., 2017. Biosens. Bioelectron. 87, 724-731.

Shandost-fard, F., Salimi, A., Khezrian, S., 2014. Biosens. Bioelectron. 53, 355-362.

Song, S., Wang, L., Li, J., Fan, C., Zhao, J., 2008. TrAC, Trends Anal. Chem. 27(2),

108-117.

Thirumalraj, B., Zhao, D.H., Chen, S.M., Palanisamy, S., 2016. J. Colloid Interface Sci. 470, 117-122.

Wang, Y.H., Xia, H., Huang, K.J., Wu, X., Ma, Y.Y., Deng, R., Lu, Y.F., Han, Z.W., 2018. Microchim. Acta 185(11), 502.

Wu, M.F., Wang, Y., Li, S., Dong, X.X., Yang, J.Y., Shen, Y.D., Wang, H., Sun, Y.M., Lei, H.T., Xu, Z.L., 2019. Anal. Chim. Acta 1049, 188-195.

Xie, Z., Lei, J., Yang, M., Li, Y., Geng, X., Liu, S., Wang, J., 2019. Biosens. Bioelectron. 127, 200-206.

Xu, W., Yi, H., Yuan, Y., Jing, P., Chai, Y., Yuan, R., Wilson, G.S., 2015a. Biosens. Bioelectron. 64, 423-428.

Xu, Y., Chu, Z., Shi, L., Peng, J., Jin, W., 2015b. Sens. Actuators, B 221, 1009-1016.

Yang, X., Ouyang, Y.J., Wu, F., Hu, Y.J., Ji, Y., Wu, Z.Y., 2017a. Sens. Actuators, B 238, 40-47.

Yang, Y., Yang, Z., Lv, J., Yuan, R., Chai, Y., 2017b. Talanta 169, 44-49.

Ye, S., Li, X., Wang, M., Tang, B., 2017. Anal. Chem. 89(9), 5124-5130.

Zhang, K., Du, Y., Chen, S., 2015. Org. Electron. 26, 380-385.

Zhang, W., Xie, G., Li, S., Lu, L., Liu, B., 2012. Appl. Surf. Sci. 258(20), 8222-8227.

Zhao, J., Zheng, T., Gao, J., Guo, S., Zhou, X., Xu, W., 2017. Analyst 142(5), 794-799.

Zhou, Y., Yu, Y.Q., Chai, Y.Q., Yuan, R., 2018. Talanta 181, 32-37.

Zhu, C.H., Zhu, W.Y., Xu, L., Zhou, X.M., 2019. Anal. Chim. Acta 1047, 21-27.

Highlights:

- A sandwich-type electrochemical aptasensor is designed for thrombin detection.
- AgNWs and hollow Au-CeO_2 are used for dual signal amplifications for the first time.
- AgNWs and hollow Au-CeO_2 show synergistic contributions to the reduction of H_2O_2
- This sandwich-type electrochemical biosensor exhibits acceptable sensitivity, stability and reproducibility for thrombin detection.

CRediT Author Statement

Qiaoxia Zhang: Methodology, Data curation, Formal analysis, Validation, Writing - original draft. **Gaochao Fan:** Data curation, Formal analysis, Validation. **Wei Chen:** Investigation, Formal analysis, Funding acquisition. **Qing Liu:** Writing - review & editing. **Xiao Zhang:** Resources. **Xianxi Zhang:** Funding acquisition. **Qingyun Liu:** Conceptualization, Writing - review & editing, Supervision, Funding acquisition, Project administration.

Declaration of interests

☒ The authors declare that they have no known competing financial interests or personal relationships that could have appeared to influence the work reported in this paper.

☐The authors declare the following financial interests/personal relationships which may be considered as potential competing interests: